

# NDNF is selectively expressed by neocortical, but not habenular neurogliaform cells

Jack F. Webster<sup>1</sup> | Rozan Vroman<sup>1</sup> | Sanne Beerens<sup>1</sup> | Shuzo Sakata<sup>1</sup> |  
Christian Wozny<sup>1,2</sup> 

<sup>1</sup>Strathclyde Institute for Pharmacy and Biomedical Sciences, University of Strathclyde, Glasgow, UK

<sup>2</sup>MSH Medical School Hamburg, Medical University, Hamburg, Germany

## Correspondence

Christian Wozny, MSH Medical School Hamburg, Medical University, Hamburg, Germany.

Email: christian.wozny@medicalschoo-hamburg.de

## Funding information

Royal Society, Grant/Award Number: Grant RG160549; Tenovus Scotland, Grant/Award Number: S16/19; Wellcome Trust, Grant/Award Number: 205917/z/17/Z; BBSRC, Grant/Award Number: BB/M00905X/1

## Abstract

The lateral habenula (LHb) is a brain structure which is known to be pathologically hyperactive in depression, whereby it shuts down the brains' reward systems. Interestingly, inhibition of the LHb has been shown to have an antidepressant effect, hence making the LHb a fascinating subject of study for developing novel antidepressant therapies. Despite this however, the exact mechanisms by which inhibitory signalling is processed within the LHb remain incompletely understood. Some studies have proposed the existence of locally targeting inhibitory interneuron populations within the LHb. One such population is believed to be akin to neocortical neurogliaform cells, yet specific molecular markers for studying these neurons are sparse and hence their function remains elusive. Recently, neuron-derived neurotrophic factor (NDNF) has been proposed as one such marker for neocortical neurogliaform cells. Using a combination of histological, physiological and optogenetic tools, we hence sought to first validate if NDNF was selectively expressed by such inhibitory neurons within the neocortex, and then if it was confined to a similar population within the LHb. While we report this to be true for the neocortex, we find no such evidence within the LHb; rather that NDNF is expressed without restriction to a particular neuronal subpopulation. These results hence indicate that molecular markers can represent broadly diverse populations of neurons on a region-to-region basis and that therefore each population as defined by molecular marker expression should be validated in each brain structure.

## 1 | INTRODUCTION

The lateral habenula (LHb) is a brain structure which is known to be hyperactive in depression (Cui et al., 2018; Li et al., 2011; Shabel et al., 2014; Yang, Cui, et al., 2018), thus potentiating inhibitory input to the midbrain reward centres (Christoph et al., 1986; Ji & Shepard, 2007; Matsumoto & Hikosaka, 2007; Wang & Aghajanian, 1977) and rendering the sufferer incapable of experiencing positive emotions

associated with these centres (Yang et al., 2018). Consequently, inhibition of the LHb has been shown to have potential as a novel therapeutic approach in the treatment of depression (Huang et al., 2019; Lecca et al., 2016; Li et al., 2011; Shabel et al., 2014; Tchenio et al., 2017; Winter et al., 2011; Yang, Cui, et al., 2018). Hence, studying the mechanisms by which inhibitory signalling is processed within the LHb should yield invaluable insight into potential treatments for depression; yet these mechanisms remain poorly understood.

Several reports have recently proposed the existence of locally targeting GABAergic neurons within the LHb (Flanigan

Edited by: Dr. Yolanda Smith

This is an open access article under the terms of the Creative Commons Attribution License, which permits use, distribution and reproduction in any medium, provided the original work is properly cited.

© 2021 The Authors. European Journal of Neuroscience published by Federation of European Neuroscience Societies and John Wiley & Sons Ltd.

et al., 2020; Webster et al., 2020; Zhang et al., 2018). Earlier work has also indicated that a subclass of neuron physiologically and morphologically akin to that of neurogliaform cells exists within the LHb (Wagner et al., 2016; Weiss & Veh, 2011), although as-of-yet no evidence exists to indicate that these form functional local connections. Neurogliaform cells are a very distinct class of inhibitory neuron known to be present in the neocortex (Olah et al., 2007; Tamás et al., 2003; Wozny & Williams, 2011), hippocampus (Armstrong et al., 2011; Price et al., 2005, 2008; Vida et al., 1998) and striatum (Ibanez-Sandoval et al., 2011). These neurons mediate both feed-forward synaptic inhibition (Armstrong et al., 2011; Price et al., 2008) and slow inhibitory signalling via volume transmission, whereby GABA spill-over from neurogliaform cell axon terminals can act on extra-synaptic GABA<sub>B</sub> receptors (Oláh et al., 2009). This permits for prolonged GABAergic signalling which can continuously dampen excitability within a large volume of neural tissue (Oláh et al., 2009; Szabadics et al., 2007). Indeed, dysfunction of GABA<sub>B</sub> signalling within the LHb is known to be implicated in driving depressive behaviour, while restoring GABA<sub>B</sub> signalling alleviates the depressive phenotype (Lecca et al., 2016). However, whether this GABA<sub>B</sub> signalling arises from local neurogliaform cell activity is still unknown. Thus, studying the local microcircuitry that these neurons form within the LHb is an intriguing prospect.

However, a problem in studying these neurons in other brain regions has been the lack of selective molecular markers (Overstreet-Wadiche & McBain, 2015). Neuropeptide Y (NPY) has classically been used as one such marker in cortical circuits (Overstreet-Wadiche & McBain, 2015; Tricoire et al., 2010), in that it is expressed by almost all neurogliaform cells, but also has the limitation that it is expressed by other neuronal populations. More recently, however, neuron-derived neurotrophic factor (NDNF) has been proposed as a more selective marker for L1 neurogliaform cells in the neocortex (Abs et al., 2018; Tasic et al., 2016; Tasic, 2018). Following up on these findings, we aimed to validate that NDNF expression was indeed selective for neurogliaform cells within the neocortex, and to then test its potential use as a marker of habenular neurogliaform cells. This would allow us to study the circuitry formed by NDNF-positive neurons within the LHb. However, we found that NDNF is expressed without restriction in LHb neurons and as such that this molecular marker is not selective for habenular neurogliaform cells as it is within the neocortex.

## 2 | MATERIALS AND METHODS

### 2.1 | Animals

All procedures were approved by the Animal Welfare and Ethical Review Body of the University of Strathclyde in accordance with UK legislation.

Male and female mice from each strain were used in this work. All animals were maintained on a C57BL/6 background, and kept on a 12:12 light/dark cycle under standard group housing conditions with unlimited access to water and normal mouse chow. New-born pups were housed with parents until weaning at P21. To generate transgenic reporter-bearing offspring, transgenic mice of the NDNF-IRES-Cre (Jax. ID 025836) (Tasic et al., 2016) or PV-IRES-Cre (Jax. ID 017320) (Hippenmeyer et al., 2005), driver lines were crossed with either Ai32 (Jax. ID 025109) (Madisen et al., 2012) or Ai9 (Jax. ID 007909) (Madisen et al., 2010) reporter mice driving expression of channelrhodopsin-2 (ChR2) and enhanced yellow fluorescent protein (eYFP), or the enhanced red fluorescent protein variant TdTomato in a Cre-dependent manner, respectively. The resulting offspring strains are hence referred to as: NDNF-IRES-Cre::Ai32 and NDNF-IRES-Cre::Ai9, or PV-IRES-Cre::Ai32. NPY-hrGFP mice (van den Pol et al., 2009) were also used in this study.

### 2.2 | Acute brain slice preparation

C57BL/6 ( $N = 5$ ; P21–28), NDNF-IRES-Cre::Ai32 ( $N = 6$ ; P21–28), NDNF-IRES-Cre::Ai9 ( $N = 5$ ; P21–36) or PV-IRES-Cre::Ai32 ( $N = 6$ ; P23–40) were humanely euthanized by cervical dislocation and immediately decapitated, and brains were rapidly removed and transferred to ice-cold oxygenated (95% O<sub>2</sub>; 5% CO<sub>2</sub>) sucrose-based artificial cerebrospinal fluid (ACSF) solution containing (in mM): sucrose 50, NaCl 87, NaHCO<sub>3</sub> 25, KCl 3, NaH<sub>2</sub>PO<sub>4</sub> 1.25, CaCl<sub>2</sub> 0.5, MgCl<sub>2</sub> 3, sodium pyruvate 3 and glucose 10. Brains sections containing the habenula were then cut in the coronal plane at 250–300  $\mu$ m on a Leica VT1200S vibratome (Leica Biosystems, Newcastle-upon-Tyne). In order to ensure slices contained the habenula, the hippocampus was used as a visual guidance due to the easily identifiable structure and immediate proximity to the habenula. Following sectioning, slices were incubated in oxygenated sucrose-based ACSF at 35°C for 30 min, and then incubated for a further 30 min at room temperature in ACSF containing (in mM) NaCl 115, NaHCO<sub>3</sub> 25, KCl 3, NaH<sub>2</sub>PO<sub>4</sub> 1.25, CaCl<sub>2</sub> 2, MgCl<sub>2</sub> 1, sodium pyruvate 3 and glucose 10. Following the incubation period, slices were stored at room temperature in oxygenated ACSF.

### 2.3 | Electrophysiological recordings

Individual slices were transferred to a recording chamber and continually perfused with oxygenated ACSF at a flow rate of 2–3 ml/min, and visualised with a Luigs and Neumann LN-Scope System (Luigs and Neumann).

The habenula is easily identifiable under differential interference contrast microscopy even at low magnification, and hence a 4× objective was used to locate the lateral habenular nucleus. A 60× objective was then used to identify suitable cells for whole-cell recordings. In the case of transgenic NDNF-IRES-Cre::Ai9, TdTomato-expressing cells could be selectively visualised with an Olympus XM10 fluorescent camera (Olympus, Southend-on-Sea) upon photostimulation with a blue LED (pE-300<sup>ultra</sup>, Cool LED, Andover, UK). Recordings were made with a Multiclamp 700B Amplifier (Molecular Devices). Glass micropipettes were filled with a solution containing (in mM) potassium gluconate 125, HEPES 10, KCl 6, EGTA 0.2, MgCl<sub>2</sub> 2, Na-ATP 2, Na-GTP 0.5, sodium phosphocreatine 5, and with 0.2% biocytin. pH was adjusted to 7.2 with KOH. For spontaneous current measurement experiments, a reduced chloride intracellular solution was used consisting of (in mM) potassium gluconate 140, potassium chloride 2, EGTA 0.2, Hepes 10, NaATP 2, NaGTP 0.5 and sodium phosphocreatine 5.

Once in whole-cell patch mode, the intrinsic properties of LHb neurons were assessed in current-clamp configuration using a stepping protocol consisting of 1-s long injections of increasing current (range: −50 to 50 pA; step size: 10 pA for LHb neurons and −500 to 500 pA; step size: 100 pA for cortical neurons). Action potential firing pattern was assessed in response to depolarizing current injection, while hyperpolarizing current injection allowed the characterisation of rebound action potential firing of neurons. Resting membrane potential (RMP) was assessed by recording the spontaneous activity of each neuron with no current injection for at least 30 s, while membrane input resistance was monitored by injecting a small hyperpolarizing pulse (100 ms; −10 to −100 pA) and measuring the voltage change. Spontaneous currents were observed in voltage clamp at a holding potential of −60 mV. Series resistance was monitored throughout. All neuronal voltage and current signals were low pass filtered at 10 kHz and acquired at 25 kHz using an ITC-18 digitizer interface (HEKA, Pfalz). The data acquisition software used was Axograph X.

## 2.4 | Optogenetic experiments and pharmacology

For optogenetic experiments, acute brain slices were prepared from transgenic NDNF-IRES-Cre::Ai32 or PV-IRES-Cre::Ai32 offspring as above in darkness. Whole-cell patch configuration was achieved, and neuronal recordings were obtained at varying holding potentials as slices were illuminated with a blue LED pulse (a single pulse

of 2 ms, power 11.5 mW) to elicit postsynaptic events. Where required, SR-95531 (2 μM; henceforth referred to as GABazine), NBQX (10 μM) or CGP-52432 (10 μM) (all from Tocris) were washed into the perfusion bath via the perfusion pump.

## 2.5 | Immunohistochemistry and neuronal recovery

Following electrophysiological recordings, slices containing neurons which had been patched and filled with biocytin were processed as previously described (Wozny & Williams, 2011). Briefly, slices were fixed overnight in 4% paraformaldehyde (PFA) dissolved in 0.1 M sodium-based phosphate-buffered saline (PBS). After fixation, slices were washed 3 × 5 min in 0.1-M PBS, and then incubated for 1 hr in a blocking solution consisting of 5% normal goat serum (NGS) and 1% Triton X-100. Slices were then allowed to incubate on a shaker at room temperature overnight in a primary antibody mixture containing 2.5% NGS and 1% Triton in PBS along with the required primary antibodies. Rabbit anti-GABA (1/200; Sigma-Aldrich) was the only primary antibody used in this study. Upon completion of the primary incubation step, slices were washed 2 × 5 min in 0.1-M PBS and incubated for 2–3 hr in a secondary antibody cocktail containing the relevant secondary antibodies along with streptavidin (conjugated to Alexa Fluor 647; 1/500 dilution; Life Technologies), in order to recover neurons which had been patched and filled with biocytin. The secondary antibodies used in this study were goat anti-rabbit conjugated to Alexa Fluor 633 or 647 (1/500 dilution; Life Technologies) and supplemented with 1% Triton in PBS. Fluorophores excitable at differing wavelengths were implicated depending on whether the slice expressed YFP (Ai32 animals) or TdTomato (Ai9 animals) to minimise crosstalk. Where only neuronal recovery was required, slices were blocked as above and incubated in a solution containing streptavidin supplemented with 1% Triton in PBS. After secondary antibody incubation, slices were washed for 3 × 5 min in 0.1-M PBS and mounted on glass slides using Vectashield medium (containing DAPI as required, Vector Labs) and cover slipped.

## 2.6 | Intracardial perfusion and serial sectioning

To prepare tissue for serial sectioning, NDNF-IRES-Cre::Ai32 (*N* = 2; P25), NDNF-IRES-Cre::Ai9 (*N* = 2; P21) or NPY-hrGFP (*N* = 2; P23) mice were terminally anaesthetized by subcutaneous injection with an

overdose cocktail of 50% lidocaine and 50% euthatal. Once anaesthetized sufficiently to be non-responsive to noxious tail and toe pinch stimuli, mice were perfused through the left ventricle with 0.1-M PBS followed by perfusion with 4% PFA dissolved in PBS. Brains were then removed and fixed overnight in 4% PFA in PBS, after which they were cryoprotected in a solution containing 30% (w/v) sucrose in PBS for storage until required for serial sectioning.

For these experiments, brains were embedded in OCT compound (VWR, Leicestershire, UK) and sectioned on a Leica SM2010 R microtome (Leica Biosystems, Newcastle upon Tyne, UK) at 60–80  $\mu\text{m}$ . Upon completion of sectioning, slices were washed  $3 \times 5$  min in 0.1-M PBS. Where further staining was required, this was carried out as above (see immunohistochemistry and neuronal recovery); however, 0.3% Triton X-100 was used in place of 1% and slices were incubated overnight in primary antibody cocktails to minimise tissue damage. Slices were then mounted using Vectashield medium (Vector Labs, Peterborough, UK) and cover slipped.

## 2.7 | Image acquisition and neuronal reconstructions

For immunohistochemistry-stained sections and biocytin-filled neurons, mounted sections were scanned on either a Leica SP5 or SP8 confocal microscope, imaging z-stacks of each slice at 2- to 4- $\mu\text{m}$  steps. Confocal laser excitation wavelengths (in nm) were 405, 488, 514 and 552. Objectives used were 10 $\times$  (dry), 20 $\times$  (oil immersion), 40 $\times$  (oil immersion) and 63 $\times$  (oil immersion) for Leica SP5, or 10 $\times$  (dry), 20 $\times$  (dry) and 63 $\times$  (oil immersion) for SP8. A zoom of up to 2 $\times$  was applied as required to occasionally visualise soma in enhanced detail. Sections were scanned to ensure that all visible streptavidin-stained cells and their neurites were included in the z-stack. 3D reconstructions of neurons were carried out using NeuTube 3D reconstruction software (Feng et al., 2015).

## 2.8 | Analysis of single-cell RNA sequencing data

The single-cell RNA sequencing data used in this paper is previously published (Hashikawa et al., 2020) and accessible via the NCBI Gene Expression Omnibus (GEO accession number: GSE137478). Information on how lateral habenula neurons were clustered was obtained from Garret Stuber's lab. Heatmaps showing the gene counts for neurogliaform cell-relevant genes were generated using MATLAB.

## 2.9 | Data analysis

Analysis of electrophysiological recordings was carried out using Axograph X. Passive intrinsic properties were calculated as described above, while active intrinsic properties (action potential initial frequency, amplitude, rise-time and half-width) were calculated by subtracting the baseline and then using the event detection feature to analysis the first action potential elicited in response to a 50-pA depolarizing pulse. For optogenetically evoked events, peak size was measured at various holding potentials. For spontaneous current measurements, representative example traces of postsynaptic currents were first generated, and currents were detected and measured using the event detection feature.

Image analysis was carried out using ImageJ. Confocal z-stacks were compressed onto a single image, and brightness and contrast were occasionally adjusted to enhance cellular visualisation. Cell counts were quantified using the cell-counter plugin. For these experiments, serial sections containing the whole habenula were imaged and analysed from one animal for each strain, and for remaining animals, every second or third section was imaged and analysed to allow quantification of markers with fair representation of the habenular subnuclei. For fluorescence intensity analysis, mean grey values of whole cells were measured in ImageJ, and normalised as relative increase over background. Background was calculated by measuring the mean grey value of an area on the slide not covered by tissue. Images were then transferred to PowerPoint (Microsoft), where cells of interest were marked.

Graphs were generated and statistical analysis was performed using GraphPad Prism 5. Statistical tests used were as follows: two-tailed unpaired *t* test for single comparisons of passive physiological properties; one-way ANOVA with Tukey's multiple comparison test for comparison of physiological properties between multiple groups; two-way ANOVA with Bonferroni's multiple comparison for assessing relationship between input current and action potential discharge (f-I analysis), or Fishers' exact test. Once graphs were generated, they were transferred to PowerPoint 2013 for formatting and assembly into figures. Statistical significance thresholds for all tests were as follows: \**p* < .05; \*\**p* < .01; and \*\*\**p* < .001. All data are provided as mean  $\pm$  SEM.

## 3 | RESULTS

### 3.1 | The LHb contains NDNF-positive neurons

To test if NDNF or NPY were also selectively expressed by neuronal subpopulations within the LHb as they are within

the neocortex (Overstreet-Wadiche & McBain, 2015; Tasic et al., 2016), we first determined whether LHB neurons did indeed express either of these markers. Sectioned slices were collected from the brains of NPY-hrGFP mice, which express GFP in NPY-positive neurons (van den Pol et al., 2009).

In these slices, while we did observe some sparse fibres in the LHB, we did not observe any NPY-positive somata (Figure 1).

Making use of publicly available data from a recently published single-cell RNA-sequencing study (Hashikawa et al., 2020), we also sought to identify if any LHB neurons contained the *Npy* RNA gene sequence. Interestingly, only very few cells from control animals did indeed contain the *Npy* gene sequence making it difficult to further examine the co-expression of other genes with *Npy*. Importantly, none of

these neurons contained the *Ndnf* or *Lamp5* gene sequences (*data not shown*); both known markers of neocortical neurogliaform cells (Tasic et al., 2018). However, to reiterate this, we have not found any fluorescently labelled somata in the NPY-hrGFP mice (Figure 1).

We next crossed NDNF-IRES-Cre mice with Ai9 reporter mice, so as to generate NDNF-IRES-Cre::Ai9 offspring ( $N = 2$ ), which expressed TdTomato in NDNF-positive neurons (Figure 2a), and imaged NDNF expression in both the somatosensory cortex (Figure 2b) and LHB (Figure 2c). Notably, NDNF was also expressed within the vasculature (Figure 2b,c; Tasic et al., 2016). While NDNF expression was largely confined to neocortical layer 1 (L1) in these slices, we also observed some expression in deeper cortical layers (Figure 2bi). Additionally, most (75.8%) but not all NDNF-positive somata co-localised with GABA (Figure 2bii), consistent with recent

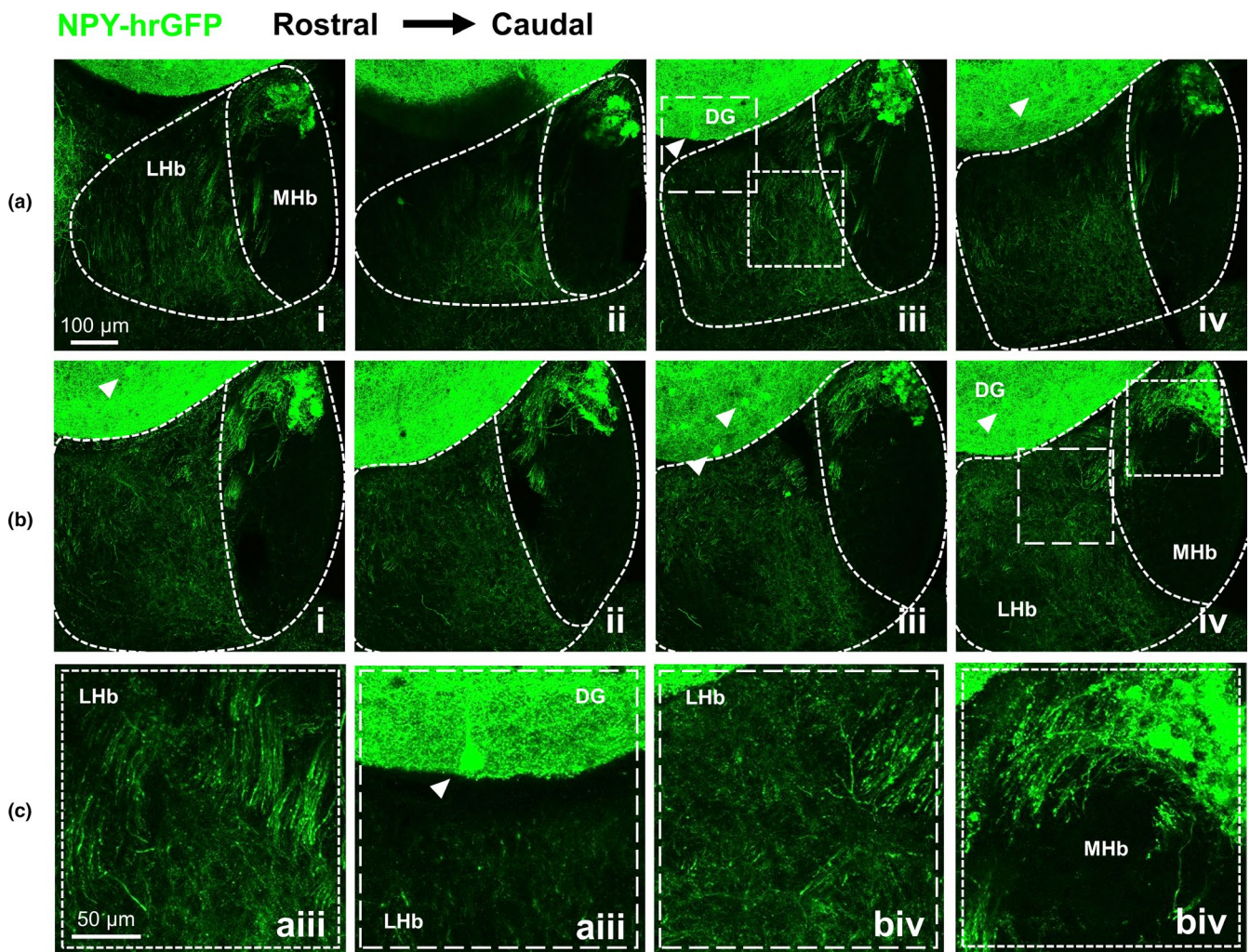


**FIGURE 1** Absence of NPY-positive neuronal somata within in the LHB. Confocal micrographs of habenular sections from NPY-hrGFP mice ( $N = 2$ ) depicting NPY-expression throughout the LHB in the rostral-caudal plane. Rows are labelled with letters ranging from (a) to (b) and columns from (i) to (iv). Magnified images from (aiii) and (biv) are displayed in row (c). Images are maximum intensity projections of 50- $\mu$ m tissue. Note that no NPY-positive somata are located within the LHB but are present in the dentate gyrus (marked by arrowheads in, e.g., aiii or bii) and in the MHb (biv, enlarged in civ). Dense NPY fibres were also observed within the dorsomedial MHb (e.g., bii). Abbreviations: DG, dentate gyrus; LHB, lateral habenula; MHb, medial habenula

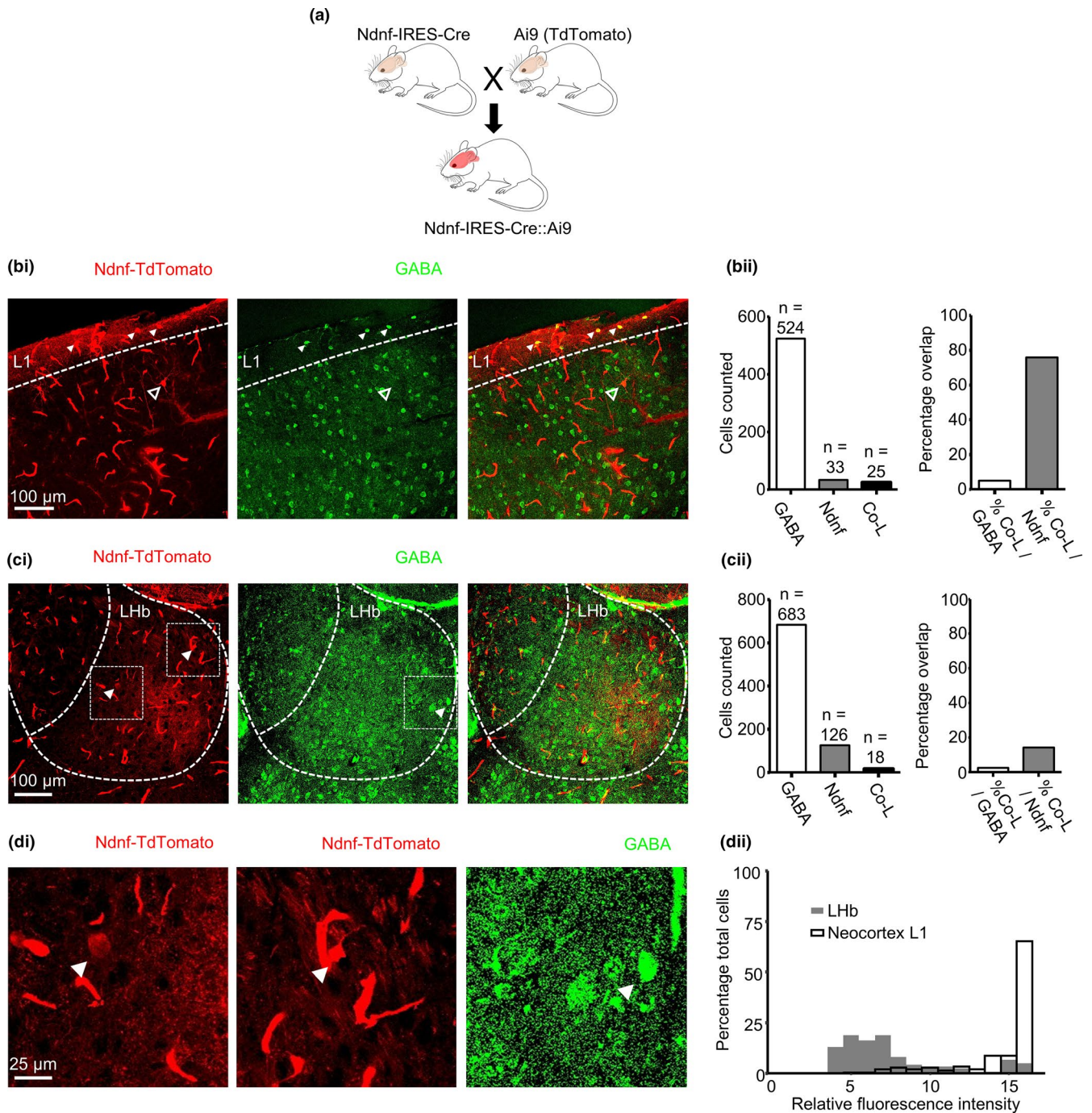


**FIGURE 2** NDNF is expressed by both neocortical and habenular neurons. (a) Schematic illustrating breeding scheme for generating NDNF-IRES-Cre::Ai9 mice. (b) Confocal micrograph depicting NDNF-positive neurons in L1 of the somatosensory cortex (arrowheads), but also a NDNF-positive neuron in the deeper somatosensory cortex which was not immunoreactive for GABA (open arrowhead). (bii) Left: bar chart quantifying total number of GABA-immunoreactive, and NDNF-positive neurons counted and the number which co-expressed both (Co-L: co-labelling;  $N = 2$  mice). Right: fraction of neurons expressing both markers as a percentage of GABA-immunoreactive neurons, and as a percentage of Ndnf-positive neurons. (c) Confocal micrograph depicting NDNF-positive neurons within the LHb (arrowheads). (cii) Left: Bar chart quantifying total number of GABA-immunoreactive, and Ndnf-positive neurons counted and the number which co-expressed both (Co-L: co-labelling;  $N = 2$  mice). Right: Fraction of neurons expressing both markers as a percentage of GABA-immunoreactive neurons, and as a percentage of NDNF-positive neurons. (d) High-resolution zoom images of the two boxed regions in (c) depicting a low fluorescence intensity LHb neuron (left), and a high fluorescence intensity LHb neuron (right). (dii) Plot illustrating distributions of relative fluorescence intensities of NDNF-positive neurons in both the LHb and L1 of the neocortex. Data are fluorescence values of cells normalised as fold increase over background fluorescence, and binned to whole number values

reports that NDNF expression is not entirely confined to L1 neurogliaform cells in the neocortex (Abs et al., 2018; Tasic et al., 2018). We did observe NDNF-positive somata within the LHb in slices from NDNF-IRES-Cre::Ai9 and NDNF-IRES-Cre::Ai32 mice (Figures 2ci and 3, respectively). However, only a small subpopulation of these (14.3%) co-localised with GABA (Figure 2cii), thus indicating that the vast majority of NDNF-positive LHb neurons are not inhibitory. Of note, we

observed that within the LHb, NDNF-positive neurons appeared to display two broadly different levels of relative fluorescence intensity (Figure 2di,dii). The majority (108 of 123; 87.8%) fluoresced relatively weakly (defined as less than a 14-fold increase in fluorescence intensity over background), while a smaller population (15 of 123; 12.2%) displayed stronger fluorescence (greater than a 14-fold increase over background; Figure 4dii). In contrast, most L1 NDNF-positive neurons (123

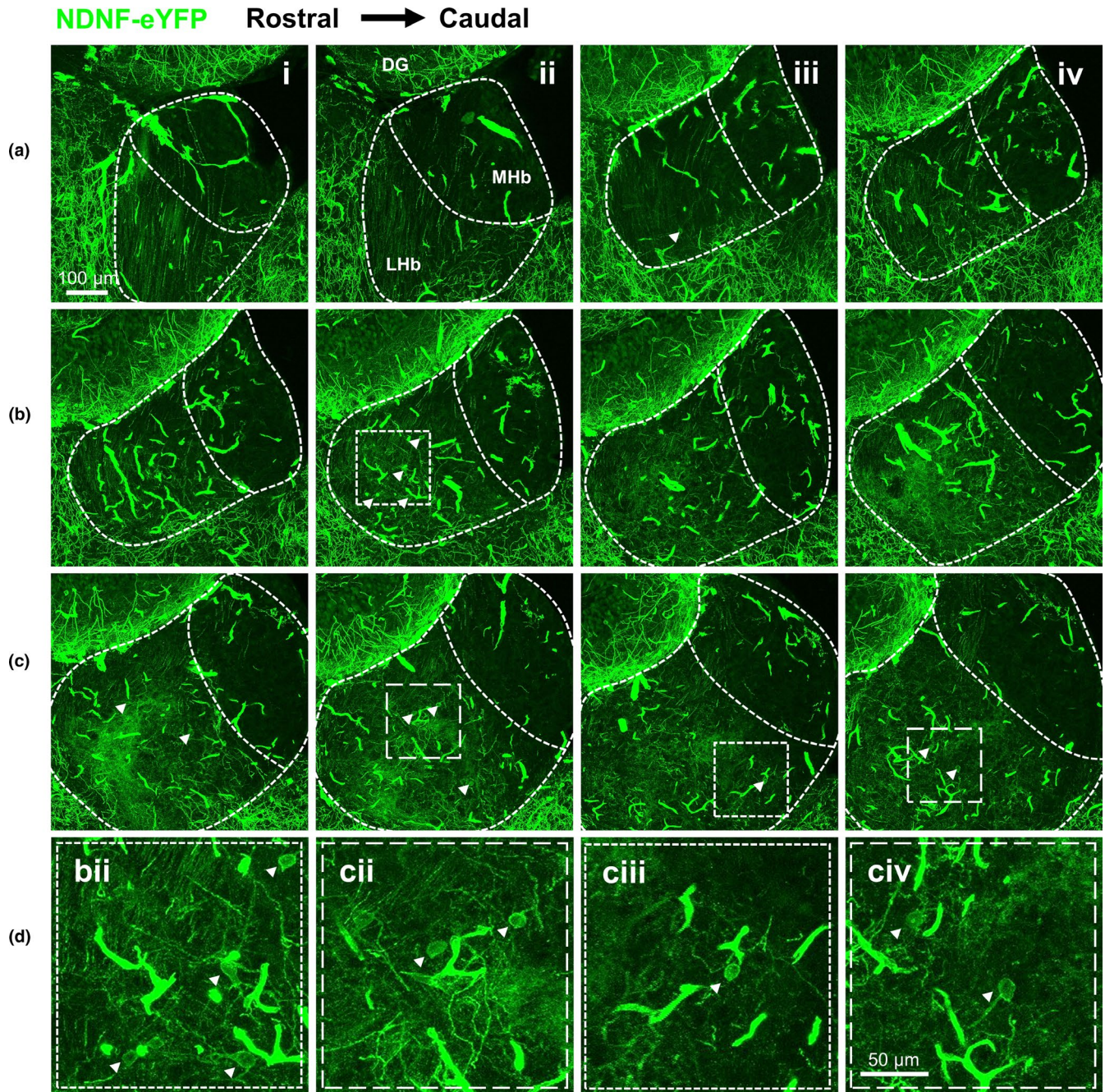


**FIGURE 3** Ndnf expression within the habenula. Rostral to caudal serial confocal micrographs illustrating NDNF expression in the habenula of an NDNF-IRES-Cre::Ai32 mouse. Arrowheads indicate NDNF-positive neurons. Rows are labelled with letters ranging from (a) to (c) and columns from (i) to (iv). Note row (d) shows higher magnification of NDNF-positive neurons taken from bii, cii – civ (neurons marked with arrowheads). Abbreviations in (a): DG, dentate gyrus; LHb, lateral habenula; MHb, medial habenula

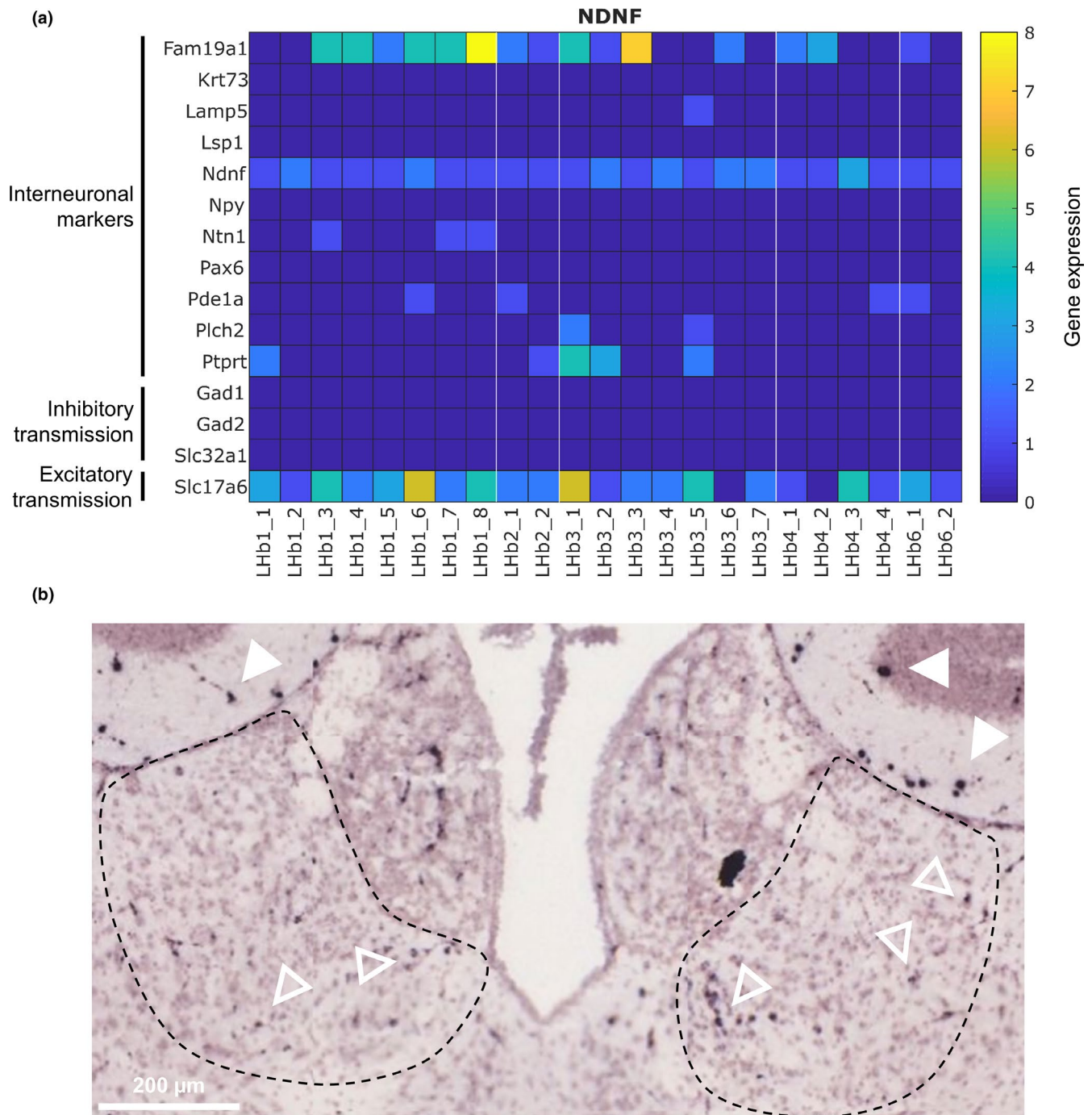


**FIGURE 4** The LHb contains neurons with *Ndnf* RNA expression. (a) Heat map depicting co-expression of *Ndnf* with genetic markers of inhibitory and excitatory transmission, and with other molecular markers known to be expressed by neocortical neurogliaform interneurons (Tasic et al., 2018). Gene expression is represented as the total number of reads for each genetic unique molecular identifier. (b) In situ hybridisation images taken from the Allen Brain Atlas depicting NDNF-positive neurons in both the LHb (open arrowheads), the adjacent dentate gyrus for comparison (closed arrowheads). Credit: <https://mouse.brain-map.org/experiment/show/72080134>

of 149; 82.6%) fell into the higher fluorescence intensity classification (Figure 2dii).

As transient developmental expression of a promoter gene can lead to full Cre-mediated recombination (Araki et al., 1995), using

Cre-mediated recombination of TdTomato as an indicator of *Ndnf* expression does not necessarily indicate the presence of NDNF-positive neurons in the adult mouse. This may serve as a possible explanation for the apparent differences in relative fluorescence intensities observed

within the NDNF-positive neurons in our data (Figure 2d). Thus, we again referred to the same previously published adult mouse single-cell RNA sequencing dataset as we did for the *Npy* gene sequence (Hashikawa et al., 2020), to ask if the adult mouse Lhb contained neurons with the *Ndnf* gene sequence (Figure 4a). From this dataset, 23 NDNF-positive cells were identified (Figure 4a). However, none of these neurons contained gene sequences for *Gad1*, *Gad2* or *Slc32a1* (Figure 4a), thus indicating that they are likely not inhibitory. Lhb neurons were clustered into six different cell types/sub-clusters: Lhb1-6 (Figure 4a); however, NDNF-positive neurons are found in all subclusters except Lhb5 (Hashikawa et al., 2020) indicating that NDNF does serve as a marker gene for a specific subgroup of neurons within the Lhb. As additional evidence in support of the existence of NDNF-positive Lhb neurons, we also searched publicly available in situ hybridisation data from the Allen Brain Atlas (<https://mouse.brain-map.org/experiment/show/72080134>). Consistently, these images also appeared to

show NDNF-positive neurons within the Lhb (Figure 4b).

Together with our histological data (Figure 2), these results indicate that the Lhb does indeed contain NDNF-positive neurons; however, most, if not all, are not inhibitory neurons.

### 3.2 | NDNF-positive neurons do not form a distinct sub-class within the Lhb

To gain an insight into the physiological characteristics of NDNF-positive Lhb neurons, we next characterised their physiological properties in acute slices from NDNF-IRES-Cre::Ai9 mice ( $n = 29$ ;  $N = 5$  mice; Figure 5). In two of these cells, action potential discharge could not be elicited upon current injection, and hence, we assumed these to be glial cells and excluded them from further analysis (Tasic et al., 2016). We assessed passive physiological properties in the remainder ( $n = 27$ ) and observed no significant difference in RMP (Figure 5b;  $n = 9$  from four mice;  $-54.6 \pm 1.3$  vs.  $-55.2 \pm 1.1$ ;  $p = .82$ ; two-tailed unpaired *t* test) or input

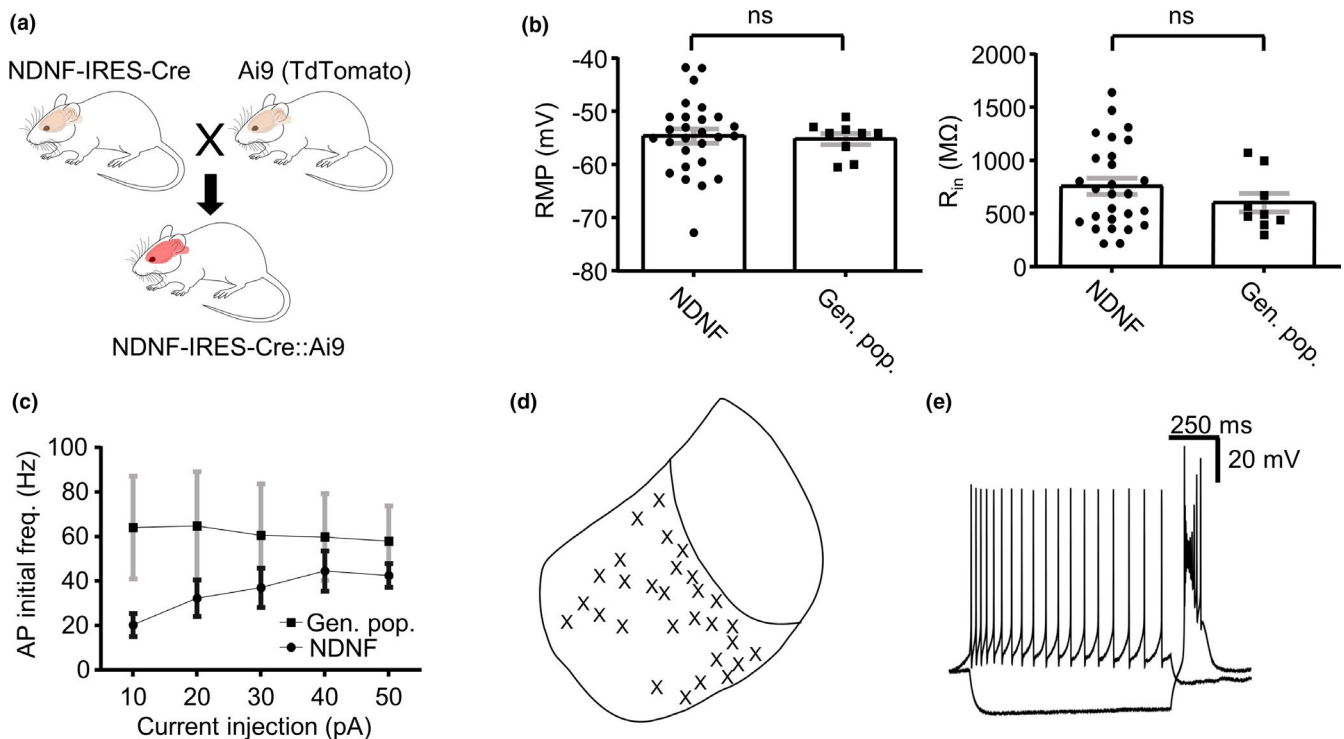


**FIGURE 5** NDNF-positive neurons do not form a distinct sub-class within the Lhb. (a) Schematic illustrating breeding scheme for generating NDNF-IRES-Cre::Ai9 mice. (b) Comparison of passive properties of NDNF-positive Lhb neurons ( $n = 27$ ;  $N = 5$  mice) and from the general population of Lhb neurons recorded in C57 mice ( $n = 9$ ;  $N = 4$  mice). Data are mean  $\pm$  SEM. (c) Comparison of firing frequency of the first induced action potential versus current injection for both NDNF-positive Lhb neurons ( $n = 23$ ;  $N = 5$  mice) and the general population of Lhb neurons ( $n = 9$ ;  $N = 4$  mice) recorded in C57 mice. Data are mean  $\pm$  SEM. (d) Schematic illustrating location of patched neurons throughout the habenular complex. (e) Example traces from a TdTomato-positive neuron in response to current injection. Current steps:  $-50$  and  $50$  pA; 1-s duration

resistance (Figure 5b;  $775.9 \pm 76.5$  vs.  $600.7 \pm 88.8$ ;  $p = .28$ ; two-tailed unpaired  $t$  test) in comparison to recordings from the general population of neurons in wild-type C57/BL6 mice. We did however observe that NDNF-positive neurons displayed a lower action potential discharge frequency in response to depolarising current injection than general population Lhb neurons (Figure 5c;  $p = .0013$ ;  $F[1, 150] = 10.71$ ; two-way ANOVA). This was a reflection of the fact that a smaller proportion of NDNF-positive neurons (4/27; 14.8%) than general population Lhb neurons (3/9; 33.3%) displayed any bursting behaviour in response to depolarising current injection (Weiss & Veh, 2011; Yang, Cui, et al., 2018). Otherwise, however, physiological properties of NDNF-positive Lhb neurons were largely consistent with previously described Lhb neuronal physiologies (Chang & Kim, 2004; Kim & Chang, 2005; Weiss & Veh, 2011) in that almost all ( $n = 22$  from 24 neurons tested) displayed rebound action potential discharge upon hyperpolarizing current injection, and a combination of tonic and bursting action potential discharge upon depolarizing current injection (Figure 5e). We also reconstructed a subset of these neurons ( $n = 5$ ) and observed that all neurons reconstructed exhibited four to six primary

dendrites, and a long unbranching axon (Figure 6), therefore lacking the characteristic axonal arbour that is a hallmark of neocortical neurogliaform cells (Overstreet-Wadiche & McBain, 2015). Again, these results hence indicate that Ndnf-positive neurons do not form a distinct subclass of neuron within the Lhb.

### 3.3 | *Ndnf* is expressed primarily by L1 inhibitory neurons within the neocortex

Having shown that *Ndnf* is expressed by primarily GABAergic and non-GABAergic neuronal populations in the neocortex and Lhb respectively (Figure 2), we sought to test whether NDNF-positive neurons mediated primarily inhibitory or excitatory transmission in each region. Hence, we next recorded photostimulation-induced postsynaptic potentials in L2/3 pyramidal neurons in acute slices from NDNF-IRES-Cre::Ai32 (Madisen et al., 2012) mice (Figure 7a;  $n = 7$  neurons;  $N = 6$  mice) in which ChR2-eYFP was expressed in NDNF-positive neurons, and observed exclusively inhibitory events in five of seven recorded neurons (Figure 7b,c). Neurogliaform

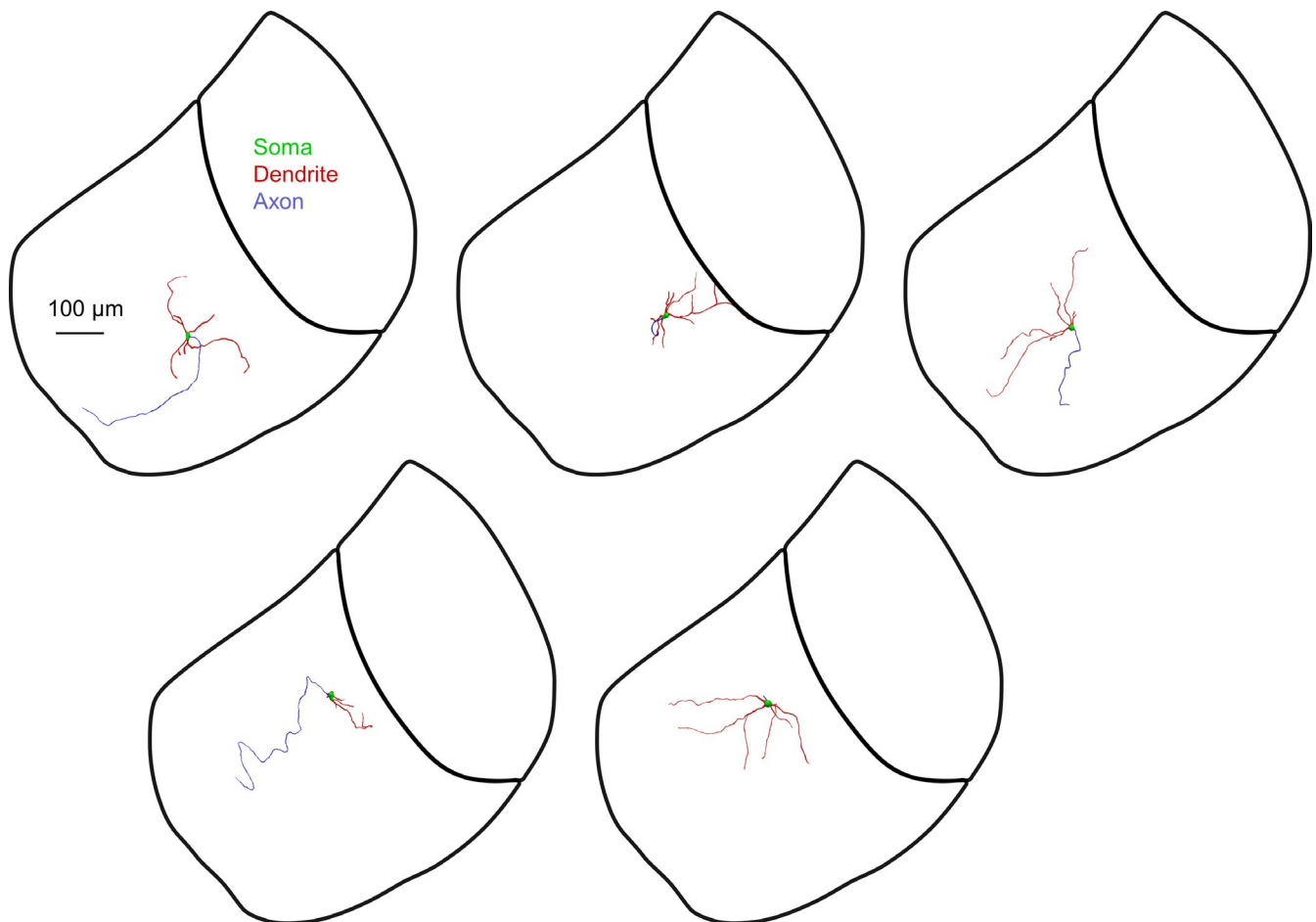


**FIGURE 6** Anatomical reconstructions from NDNF-positive neurons. Example reconstructions from five NDNF-positive neurons. Note that each neuron contains an unbranching axon, possibly indicative of a projection neuron

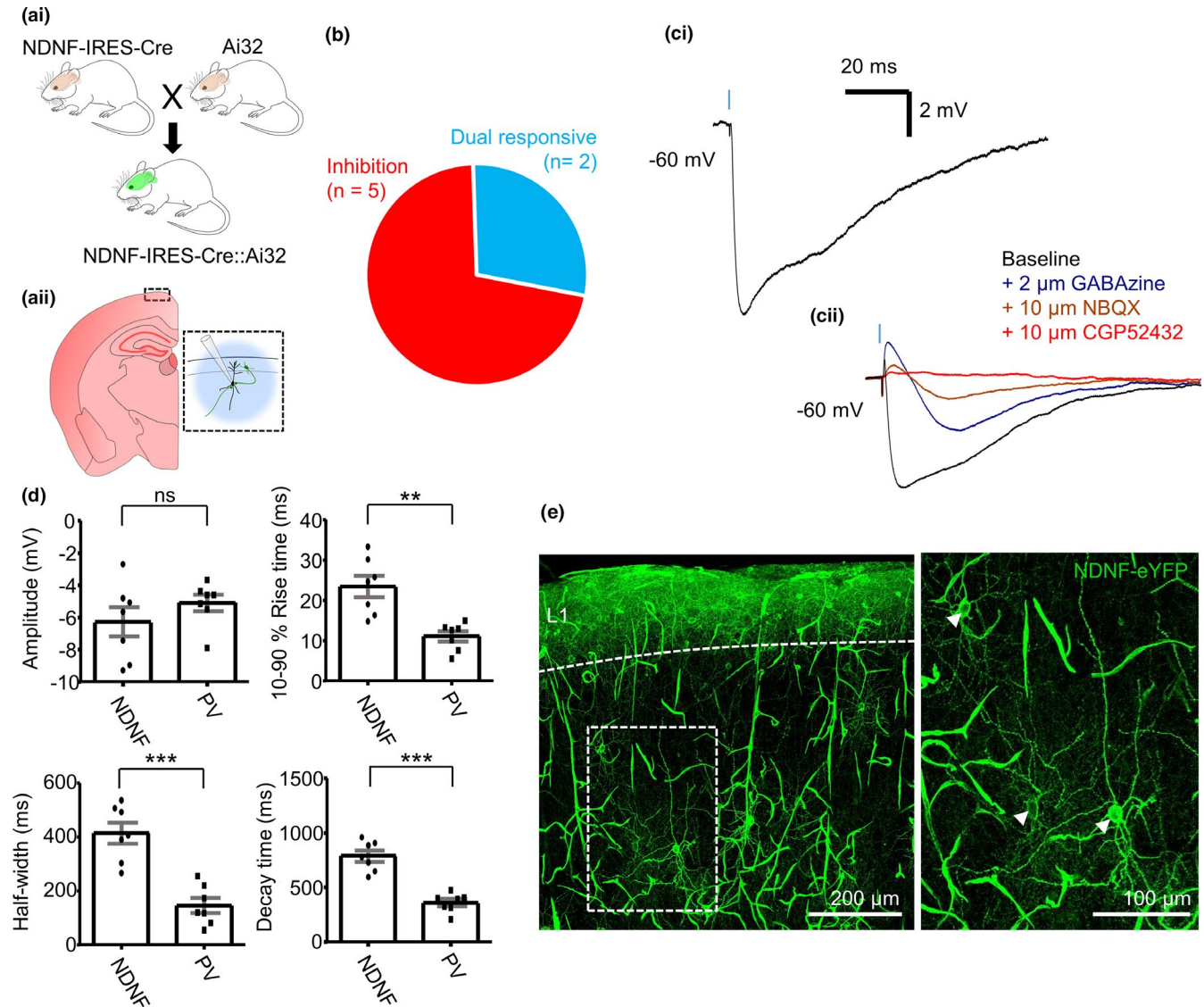


**FIGURE 7** *Ndnf* is expressed primarily by L1 inhibitory neurons in the somatosensory cortex. (a i) Schematic illustrating breeding scheme for generating NDNF-IRES-Cre::Ai32 mice. (a ii) Schematic of recording scheme. L2/3 pyramidal neurons were patched, and blue light was used to stimulate both local and long-distance NDNF-positive neurons. (b) Pie chart quantifying nature of postsynaptic potentials elicited in response to photostimulation.  $n = 7$  neurons. (c) Example traces from a neuron displaying an IPSP in response to photostimulation (cii) Example traces from a neuron in which an NBQX-sensitive EPSP was unmasked upon application of GABA<sub>A</sub>. The leftover GABA<sub>B</sub>-component was removed by CGP52432, a selective GABA<sub>B</sub> receptor antagonist (d) Scatter plots comparing amplitude and kinetics of photostimulation-induced IPSPs in NDNF-IRES-Cre::Ai32 slices versus PV-IRES-Cre::Ai32 slices. (e) Left: Confocal micrograph depicting localization of NDNF-positive neurons in the somatosensory cortex. Right: Zoom-in of the boxed region showing NDNF-positive neurons not located within neocortical L1 (arrowheads)

cells are known to mediate slow inhibition, with IPSPs mediated by these neurons having larger GABA<sub>B</sub> components (Price et al., 2005, 2008; Tamás et al., 2003; Wozny & Williams, 2011). Therefore, we also expressed ChR2 in PV-positive neurons (termed PV-IRES-Cre::Ai32 mice) and compared L2/3 pyramidal neuron IPSPs in NDNF-IRES-Cre::Ai32 slices to those in PV-IRES-Cre::Ai32 slices (Figure 7d;  $n = 7$  neurons;  $N = 6$  mice) upon photostimulation. Consistently, we observed large IPSPs with comparable amplitude ( $-6.3 \pm 0.9$  mV vs.

$-5.1 \pm 0.5$  mV for NDNF- vs. PV-positive neurons;  $p = .29$ ; two-tailed unpaired  $t$  test) in both lines, but with slower kinetics (rise time  $23.5 \pm 2.7$  ms vs.  $11.1 \pm 1.3$  ms;  $p = .001$ ; half-width  $414.6 \pm 39.1$  ms vs.  $146.0 \pm 27.6$  ms;  $p = .0001$ ; decay  $787.4 \pm 51.9$  ms vs.  $361.3 \pm 32.8$  ms;  $p < .0001$  for NDNF- vs. PV-positive neurons respectively; two-tailed unpaired  $t$  test) in the NDNF-IRES-Cre::Ai32 slices (Figure 7d) indicative of a large GABA<sub>B</sub> component. Interestingly, in two neurons from NDNF-IRES-Cre::Ai32 slices, GABA<sub>A</sub> and GABA<sub>B</sub> blockade unmasked a small AMPA-mediated

excitatory component (Figure 7cii). As with the NDNF-IRES-Cre::Ai9 line, post hoc confocal imaging of these slices also revealed some NDNF-positive somata outside of L1 (Figure 2e), hence confirming findings from recent reports (Abs et al., 2018; Tasic et al., 2016, 2018) that *Ndnf* is largely, but not exclusively, confined to neocortical L1 inhibitory neurons; which based on the slow GABA<sub>B</sub> signalling they mediate (Figure 7c,d), are presumably neurogliaform cells (Oláh et al., 2009; Tamás et al., 2003; Wozny & Williams, 2011).

### 3.4 | NDNF-positive neurons mediate primarily excitatory transmission within the LHb

Finally, to examine whether *Ndnf*-positive axonal fibres elicit excitatory or inhibitory transmission within the LHb, we recorded from LHb neurons in slices from NDNF-IRES-Cre::Ai32 mice while photostimulating NDNF-positive neurons (Figure 8a;  $n = 21$  neurons from six mice). In the LHb, most responsive neurons ( $n = 5$  of 6) displayed a solely excitatory postsynaptic potential (Figure 8b,ci), while one neuron displayed a postsynaptic potential with both an NBQX-sensitive excitatory component and a GABA<sub>A</sub>-sensitive inhibitory component (Figure 8cii). These responses were spread fairly evenly throughout the LHb (Figure 8d), consistent with confocal imaging of serial coronal sections from NDNF-IRES-Cre::Ai32 mice ( $N = 2$ ), in that both

NDNF-positive fibres and somata were dispersed evenly throughout the LHb (Figure 3). Altogether, these results suggest that while NDNF is largely confined to L1 inhibitory neurons within the neocortex which are presumably neurogliaform cells, we find that within the LHb, NDNF is not expressed selectively by any subclass of LHb neuron.

## 4 | DISCUSSION

Consistent with recent reports (Abs et al., 2018; Tasic et al., 2016, 2018), we find that *Ndnf* is expressed mostly, but not exclusively, by inhibitory L1 neurons within the neocortex. However, within the LHb we report that *Ndnf* does not act as a selective marker for any subpopulation of inhibitory neuron and instead report that the majority of input to LHb neurons from NDNF-positive neurons is excitatory.

### 4.1 | An absence of markers for studying the role of neurogliaform cells in the LHb

Selective markers for studying the role of inhibitory neurogliaform cells in cortical circuits have been sparse (Overstreet-Wadiche & McBain, 2015), and we thus sought to validate the use of *Ndnf* as such a marker in the somatosensory cortex (Tasic et al., 2016). Our results are consistent with other recent reports (Abs et al., 2018; Tasic et al., 2018) in that we find *Ndnf* to be mostly, but not

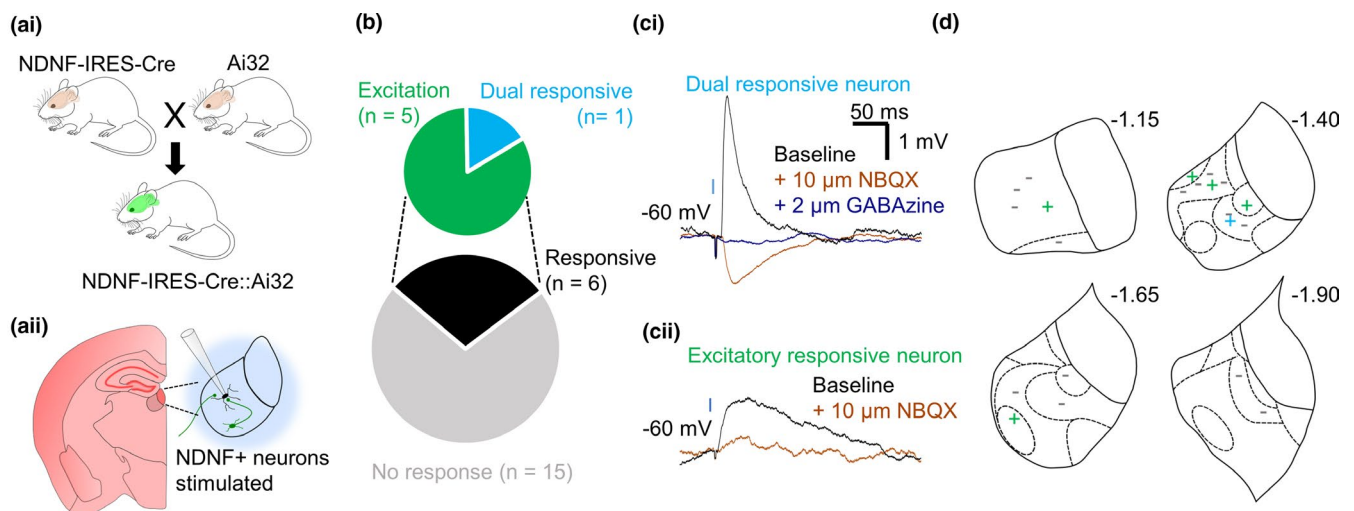


**FIGURE 8** NDNF-positive neurons mediate primarily excitatory transmission within the LHb. (ai) Schematic illustrating breeding scheme for generating NDNF-IRES-Cre::Ai32 mice. (aia) Schematic of recording scheme. LHb neurons were patched and blue light was used to stimulate both local and long-distance NDNF-positive neurons. (b) Pie chart quantifying fraction of neurons responsive to photostimulation, and the nature of those responses. (ci) Example traces from two separate neurons in which photostimulation elicited a response with both an NBQX-sensitive excitatory component, and a GABA<sub>A</sub>-sensitive inhibitory component (cii) Example traces from a neuron in which photostimulation elicited an excitatory response (bottom). (d) Schematic illustrating locations of patched neurons within the habenular complex, projected rostrally (top left) through caudally (bottom right). Non-responsive neurons are indicated by—(grey bar), while responsive neurons are indicated by + EPSP only (green plus); + dual response (light blue plus)

exclusively, confined to inhibitory neurons which mediate inhibitory transmission through both GABA<sub>A</sub> and GABA<sub>B</sub> receptors (Figures 2 and 7). In contrast, we find no such evidence in the LHb (Figures 2, 4 and 8). Consistently, we observed no neuronal somata positive for NPY (Figure 1). Therefore, our results do not support the notion of the existence of neurogliaform cells within the LHb (Wagner et al., 2016; Weiss & Veh, 2011), or at least not those with similar molecular marker expression to those described in the neocortex (Abs et al., 2018; Tasic et al., 2016, 2018). However, these previous works were carried out in rat; hence, we cannot exclude that this discrepancy is simply a species difference. Therefore, while it is therefore possible that neurogliaform cells are present within the mouse LHb, we conclude that neither *Ndnf* nor *Npy* can be used as a marker to study them.

## 4.2 | The association between molecular marker expression and neuronal classification

This lack of neurogliaform cell specificity of *Ndnf* and *Npy* in the LHb is in contrast to the neocortex (Abs et al., 2018; Overstreet-Wadiche & McBain, 2015; Tasic et al., 2016, 2018; Tricoire et al., 2010). This then raises an interesting point of discussion regarding whether a neuron can truly be classified into a distinct subpopulation based on gene expression. Indeed, molecular marker expression has classically been thought of as one of the key criteria for defining populations of interneurons (Ascoli et al., 2008). However, the presence of these neurons within the LHb has previously been proposed based on a similar morphological and physiological profile to those in the neocortex (Wagner et al., 2016; Weiss & Veh, 2011). Therefore, if the genetic profile of such a neuron were to be entirely different to its neocortical counterpart, one could argue that it may be an entirely different subpopulation of neuron. This can be complicated further by the matter that there is still debate as to the criteria by which neurogliaform cells can be differentiated from other L1 neurons within the neocortex (Schuman et al., 2019). Therefore, a clearer definition of these neurons is still required, as are more selective markers. Meeting these conditions will permit studying the circuitry and function of these neurons in far greater detail both within the neocortex and the LHb, and perhaps future work may reveal that these proposed LHb neurogliaform cells are in fact an entirely novel subclass of inhibitory neuron altogether.

## 5 | CONCLUSIONS

We have investigated the physiological and histological properties of NDNF-positive neurons within the neocortex

and LHb and characterised the nature of transmission mediated by these neurons in each region. While we report that *Ndnf* is largely confined to L1 inhibitory neurons within the neocortex, we find no such evidence within the LHb, finding instead that *Ndnf* is expressed largely without restriction to a particular subclass of neuron. These results hence indicate that molecular markers can represent broadly diverse populations of neurons on a region-to-region basis, and therefore, these populations must be validated in each region.

## ACKNOWLEDGEMENTS

We thank Peer Wulff for insightful discussions and critical comments on an earlier version of the manuscript. We are also grateful to Hongkui Zeng from the Allen Brain Institute, Seattle, for kindly sharing the Ai9 reporter mice with us, and we thank Csaba Földy, Brain Research Institute, University of Zurich, Switzerland, for generously providing us with NPY-hrGFP mice. In addition, we would like to acknowledge the help of Yoshiko Hashikawa, Koichi Hashikawa, and Garret Stuber for sharing their data and the cluster analysis of lateral habenula neurons. The work was supported by the Royal Society (Research Grant RG160549, CW), Tenovus Scotland (Project S16/19, CW), the Wellcome Trust (205917/z/17/Z, CW), and the BBSRC (BB/M00905X/1, SS). JFW held a studentship funded by the Engineering and Physical Sciences Research Council (EPSRC).

## CONFLICT OF INTEREST

The authors declare no conflict of interest.

## AUTHOR CONTRIBUTIONS

CW designed the research; JFW and RV performed the research; JFW and SB analysed the data; SS contributed to the tools; JFW and CW Wrote the paper with the help of RV and SS.

## PEER REVIEW

The peer review history for this article is available at <https://publons.com/publon/10.1111/ejn.15237>.

## DATA AVAILABILITY STATEMENT

All data can be obtained upon request to the corresponding author.

## ORCID

Christian Wozny  <https://orcid.org/0000-0003-4220-2033>

## REFERENCES

- Abs, E., Poorthuis, R. B., Apelblat, D., Muhammad, K., Pardi, M. B., Enke, L., Kushinsky, D., Pu, D. L., Eizinger, M. F., Conzelmann, K. K., Spiegel, I., & Letzkus, J. J. (2018). Learning-related plasticity in dendrite-targeting layer 1 interneurons. *Neuron*, *100*, 684–699. <https://doi.org/10.1016/j.neuron.2018.09.001>

- Araki, K., Araki, M., Miyazaki, J. I., & Vassalli, P. (1995). Site-specific recombination of a transgene in fertilized eggs by transient expression of Cre recombinase. *Proceedings of the National Academy of Sciences*, *92*, 160–164. <https://doi.org/10.1073/pnas.92.1.160>
- Armstrong, C., Szabadics, J., Tamas, G., & Soltesz, I. (2011). Neurogliaform cells in the molecular layer of the dentate gyrus as feed-forward GABAergic modulators of entorhino-hippocampal interplay. *The Journal of Comparative Neurology*, *519*, 1476–1491.
- Ascoli, G. et al (2008). Petilla terminology: Nomenclature of features of GABAergic interneurons of the cerebral cortex. *Nature Reviews Neuroscience*, *9*, 557–568.
- Chang, S., & Kim, U. (2004). Ionic mechanism of long-lasting discharges of action potentials triggered by membrane hyperpolarization in the medial lateral habenula. *Journal of Neuroscience*, *24*, 2172–2181. <https://doi.org/10.1523/JNEUROSCI.4891-03.2004>
- Christoph, G. R., Leonzio, R. J., & Wilcox, K. S. (1986). Stimulation of the lateral habenula inhibits dopamine-containing neurons in the substantia nigra and ventral tegmental area of the rat. *Journal of Neuroscience*, *6*, 613–619. <https://doi.org/10.1523/JNEUROSCI.06-03-00613.1986>
- Cui, Y., Yang, Y., Ni, Z., Dong, Y., Cai, G., Foncelle, A., Ma, S., Sang, K., Tang, S., Li, Y., Shen, Y., Berry, H., Wu, S., & Hu, H. (2018). Astroglial Kir4.1 in the lateral habenula drives neuronal bursts in depression. *Nature*, *554*, 323–327. <https://doi.org/10.1038/nature25752>
- Feng, L., Zhao, T., & Kim, J. (2015). neuTube 1.0: a new design for efficient neuron reconstruction software based on the SWC format. *Eneuro*, *2*(1), ENEURO.0049-14.2014. <https://doi.org/10.1523/ENEURO.0049-14.2014>
- Flanigan, M. E., Aleyasin, H., Li, L., Burnett, C. J., Chan, K. L., LeClair, K. B., Lucas, E. K., Matikainen-Ankney, B., Durand-de Cuttoli, R., Takahashi, A., Menard, C., Pfau, M. L., Golden, S. A., Bouchard, S., Calipari, E. S., Nestler, E. J., DiLeone, R. J., Yamanaka, A., Huntley, G. W., ... Russo, S. J. (2020). Orexin signaling in GABAergic lateral habenula neurons modulates aggressive behavior in male mice. *Nature Neuroscience*, *23*, 638–650. <https://doi.org/10.1038/s41593-020-0617-7>
- Hashikawa, Y., Hashikawa, K., Rossi, M. A., Johnston, N. L., Ahmad, O. R., Stuber, G. D., Hashikawa, Y., Hashikawa, K., Rossi, M. A., Basiri, M. L., Liu, Y., & Johnston, N. L. (2020). Transcriptional and Spatial Resolution of Cell Types in the Mammalian Habenula NeuroResource Transcriptional and Spatial Resolution of Cell Types in the Mammalian Habenula. *Neuron*, *1–16*, <https://doi.org/10.1016/j.neuron.2020.03.011>
- Hippenmeyer, S., Vrieseling, E., Sigrist, M., Portmann, T., Laengle, C., Ladle, D. R., & Arber, S. (2005). A developmental switch in the response of DRG neurons to ETS transcription factor signaling. *PLoS Biology*, *3*, 0878–0890. <https://doi.org/10.1371/journal.pbio.0030159>
- Huang, L., Xi, Y., Peng, Y., Yang, Y., Huang, X., Fu, Y., Tao, Q., Xiao, J., Yuan, T., An, K., Zhao, H., Pu, M., Xu, F., Xue, T., Luo, M., So, K., & Ren, C. (2019). A visual circuit related to habenula underlies the antidepressive effects of light therapy. *Neuron*, *102*, 128–142. <https://doi.org/10.1016/j.neuron.2019.01.037>
- Ibanez-Sandoval, O., Tecuapetla, F., Unal, B., Shah, F., Koos, T., & Tepper, J. M. (2011). A Novel functionally distinct subtype of striatal neuropeptide Y interneuron. *Journal of Neuroscience*, *31*, 16757–16769. <https://doi.org/10.1523/JNEUROSCI.2628-11.2011>
- Ji, H., & Shepard, P. D. (2007). Lateral habenula stimulation inhibits rat midbrain dopamine neurons through a GABA(A) receptor-mediated mechanism. *Journal of Neuroscience*, *27*, 6923–6930. <https://doi.org/10.1523/JNEUROSCI.0958-07.2007>
- Kim, U., & Chang, S. Y. (2005). Dendritic morphology, local circuitry, and intrinsic electrophysiology of neurons in the rat medial and lateral habenular nuclei of the epithalamus. *The Journal of Comparative Neurology*, *483*, 236–250. <https://doi.org/10.1002/cne.20410>
- Lecca, S., Pelosi, A., Tchenio, A., Moutkine, I., Lujan, R., Hervé, D., & Mameli, M. (2016). Rescue of GABAB and GIRK function in the lateral habenula by protein phosphatase 2A inhibition ameliorates depression-like phenotypes in mice. *Nature Medicine*, *22*, 254–261. <https://doi.org/10.1038/nm.4037>
- Li, B., Piriz, J., Mirrione, M., Chung, C., Proulx, C. D., Schulz, D., Henn, F., & Malinow, R. (2011). Synaptic potentiation onto habenula neurons in the learned helplessness model of depression. *Nature*, *470*, 535–539. <https://doi.org/10.1038/nature09742>
- Madisen, L., Mao, T., Koch, H., Zhuo, J.-M., Berenyi, A., Fujisawa, S., Hsu, Y.-W., Garcia, A. J., Gu, X., Zanella, S., Kidney, J., Gu, H., Mao, Y., Hooks, B. M., Boyden, E. S., Buzsáki, G., Ramirez, J. M., Jones, A. R., Svoboda, K., ... Zeng, H. (2012). A toolbox of Cre-dependent optogenetic transgenic mice for light-induced activation and silencing. *Nature Neuroscience*, *15*, 793–802. <https://doi.org/10.1038/nn.3078>
- Madisen, L., Zwingman, T. A., Sunkin, S. M., Oh, S. W., Zariwala, H. A., Gu, H., Ng, L. L., Palmiter, R. D., Hawrylycz, M. J., Jones, A. R., Lein, E. S., & Zeng, H. (2010). A robust and high-throughput Cre reporting and characterization system for the whole mouse brain. *Nature Neuroscience*, *13*, 133–140. <https://doi.org/10.1038/nn.2467>
- Matsumoto, M., & Hikosaka, O. (2007). Lateral habenula as a source of negative reward signals in dopamine neurons. *Nature*, *447*, 1111–1115. <https://doi.org/10.1038/nature05860>
- Oláh, S., Füle, M., Komlósi, G., Varga, C., Báldi, R., Barzó, P., & Tamás, G. (2009). Regulation of cortical microcircuits by unitary GABA-mediated volume transmission. *Nature*, *461*, 1278–1281. <https://doi.org/10.1038/nature08503>
- Olah, S., Komlosi, G., Szabadics, J., Varga, C., Toth, E., Barzo, P., & Tamas, G. (2007). Output of neurogliaform cells to various neuron types in the human and rat cerebral cortex. *Frontiers in Neural Circuits*, *1*. <https://doi.org/10.3389/neuro.04.004.2007>
- Overstreet-Wadiche, L., & McBain, C. J. (2015). Neurogliaform cells in cortical circuits. *Nature Reviews Neuroscience*, *16*, 458–468. <https://doi.org/10.1038/nrn3969>
- Price, C. J., Cauli, B., Kovacs, E. R., Kulik, A., Lambolez, B., Shigemoto, R., & Capogna, M. (2005). Neurogliaform Neurons Form a Novel Inhibitory Network in the Hippocampal CA1 Area. *Journal of Neuroscience*, *25*, 6775–6786. <https://doi.org/10.1523/JNEUROSCI.1135-05.2005>
- Price, C. J., Scott, R., Rusakov, D. A., & Capogna, M. (2008). GABA(B) receptor modulation of feedforward inhibition through hippocampal neurogliaform cells. *Journal of Neuroscience*, *28*, 6974–6982. <https://doi.org/10.1523/JNEUROSCI.4673-07.2008>
- Schuman, B., Machold, R. P., Hashikawa, Y., Fuzik, J., Fishell, G. J., & Rudy, B. (2019). Four Unique interneuron populations reside in neocortical layer 1. *Journal of Neuroscience*, *39*, 125–139. <https://doi.org/10.1523/JNEUROSCI.1613-18.2018>
- Shabel, S. J., Proulx, C. D., Piriz, J., & Malinow, R. (2014). Mood regulation. GABA/glutamate co-release controls habenula output and

- is modified by antidepressant treatment. *Science*, 345, 1494–1498. <https://doi.org/10.1126/science.1250469>
- Shabel, S. J., Proulx, C. D., Piriz, J., & Manilow, R. (2014). Mood regulation. GABA/glutamate co-release controls habenula output and is modified by antidepressant treatment. *Science*, 345, 1494–1498. <https://doi.org/10.1126/science.1250469>
- Szabadics, J., Tamás, G., & Soltesz, I. (2007). Different transmitter transients underlie presynaptic cell type specificity of GABA<sub>A</sub>, slow and GABA<sub>A</sub>, fast. *Proceedings of the National Academy of Sciences*, 104, 14831–14836. <https://doi.org/10.1073/pnas.0707204104>
- Tamás, G., Lorincz, A., Simon, A., & Szabadics, J. (2003). Identified sources and targets of slow inhibition in the neocortex. *Science*, 299(5614), 1902–1905. <https://doi.org/10.1126/science.1082053>
- Tasic, B., Menon, V., Nguyen, T. N., Kim, T. K., Jarsky, T., Yao, Z., Levi, B., Gray, L. T., Sorensen, S. A., Dolbeare, T., Bertagnolli, D., Goldy, J., Shapovalova, N., Parry, S., Lee, C., Smith, K., Bernard, A., Madisen, L., Sunkin, S. M., ... Zeng, H. (2016). Adult mouse cortical cell taxonomy revealed by single cell transcriptomics. *Nature Neuroscience*, 19, 335–346. <https://doi.org/10.1038/nn.4216>
- Tasic, B., Yao, Z., Graybuck, L. T., Smith, K. A., Nguyen, T. N., Bertagnolli, D., Goldy, J., Garren, E., Economo, M. N., Viswanathan, S., Penn, O., Bakken, T., Menon, V., Miller, J., Fong, O., Hirokawa, K. E., Lathia, K., Rimorin, C., Tieu, M., ... Zeng, H. (2018). Shared and distinct transcriptomic cell types across neocortical areas. *Nature*, 563, 72–78. <https://doi.org/10.1038/s41586-018-0654-5>
- Tchenio, A., Lecca, S., Valentinova, K., & Mameli, M. (2017). Limiting habenular hyperactivity ameliorates maternal separation-driven depressive-like symptoms. *Nature Communications*, 8, 1135. <https://doi.org/10.1038/s41467-017-01192-1>
- Tricoire, L., Pelkey, K. A., Daw, M. I., Sousa, V. H., Miyoshi, G., Jeffries, B., Cauli, B., Fishell, G., & McBain, C. J. (2010). Common origins of hippocampal Ivy and nitric oxide synthase expressing neurogliaform cells. *Journal of Neuroscience*, 30, 2165–2176. <https://doi.org/10.1523/JNEUROSCI.5123-09.2010>
- van den Pol, A. N., Yao, Y., Fu, L.-Y., Foo, K., Huang, H., Coppari, R., Lowell, B. B., & Broberger, C. (2009). Neuromedin B and gastrin-releasing peptide excite arcuate nucleus neuropeptide Y neurons in a novel transgenic mouse expressing strong renilla green fluorescent protein in NPY neurons. *Journal of Neuroscience*, 29, 4622–4639. <https://doi.org/10.1523/JNEUROSCI.3249-08.2009>
- Vida, I., Halasy, K., Szinyei, C., Somogyi, P., & Buhl, E. H. (1998). Unitary IPSPs evoked by interneurons at the stratum radiatum-stratum lacunosum-moleculare border in the CA1 area of the rat hippocampus in vitro. *Journal of Physiology*, 506, 755–773.
- Wagner, F., Bernard, R., Derst, C., French, L., & Veh, R. W. (2016). Microarray analysis of transcripts with elevated expressions in the rat medial or lateral habenula suggest fast GABAergic excitation in the medial habenula and habenular involvement in the regulation of feeding and energy balance. *Brain Structure and Function*, 221, 4463–4489. <https://doi.org/10.1007/s00429-016-1195-z>
- Wang, R. Y., & Aghajanian, G. K. (1977). Physiological evidence for habenula as major link between forebrain and midbrain raphe. *Science*, 197, 89–91. <https://doi.org/10.1126/science.194312>
- Webster, J. F., Vroman, R., Balueva, K., Wulff, P., Sakata, S., & Wozny, C. (2020). Disentangling neuronal inhibition and inhibitory pathways in the lateral habenula. *Scientific Reports*, 10, 1–17. <https://doi.org/10.1038/s41598-020-65349-7>
- Weiss, T., & Veh, R. W. (2011). Morphological and electrophysiological characteristics of neurons within identified subnuclei of the lateral habenula in rat brain slices. *Neuroscience*, 172, 74–93. <https://doi.org/10.1016/j.neuroscience.2010.10.047>
- Winter, C., Vollmayr, B., Djodari-Irani, A., Klein, J., & Sartorius, A. (2011). Pharmacological inhibition of the lateral habenula improves depressive-like behavior in an animal model of treatment resistant depression. *Behavioral Brain Research*, 216, 463–465. <https://doi.org/10.1016/j.bbr.2010.07.034>
- Wozny, C., & Williams, S. R. (2011). Specificity of synaptic connectivity between layer 1 inhibitory interneurons and layer 2/3 pyramidal neurons in the rat neocortex. *Cerebral Cortex*, 21, 1818–1826. <https://doi.org/10.1093/cercor/bhq257>
- Yang, Y., Cui, Y., Sang, K., Dong, Y., Ni, Z., Ma, S., & Hu, H. (2018). Ketamine blocks bursting in the lateral habenula to rapidly relieve depression. *Nature*, 554, 317–322. <https://doi.org/10.1038/nature25509>
- Yang, Y., Wang, H., Hu, J., & Hu, H. (2018). Lateral habenula in the pathophysiology of depression. *Current Opinion in Neurobiology*, 48, 90–96. <https://doi.org/10.1016/j.conb.2017.10.024>
- Zhang, L., Hernández, V. S., Swinny, J. D., Verma, A. K., Giesecke, T., Emery, A. C., Mutig, K., Garcia-Segura, L. M., & Eiden, L. E. (2018). A GABAergic cell type in the lateral habenula links hypothalamic homeostatic and midbrain motivation circuits with sex steroid signaling. *Translational Psychiatry*, 8, 50. <https://doi.org/10.1038/s41398-018-0099-5>

**How to cite this article:** Webster JF, Vroman R, Beerens S, Sakata S, Wozny C. NDNF is selectively expressed by neocortical, but not habenular neurogliaform cells. *Eur J Neurosci*. 2021;00:1–15. <https://doi.org/10.1111/ejn.15237>